PCCP

Accepted Manuscript

ROYAL SOCIETY OF CHEMISTRY

www.rsc.org/pccp

Gold Nanoparticle Array Formation on Dimpled Ta Templates Using Pulsed Laser-Induced Thin Film Dewetting

Hany A. El-Sayed[1], Corie A. Horwood, Ebenezer Owusu-Ansah, Yujun J. Shi and Viola I. Birss*

Department of Chemistry, University of Calgary, Calgary, Alberta, Canada T2N 1N4

[1] Permanent address: National Research Center, Dokki, Cairo, Egypt.

* Corresponding author: (Email: birss@ucalgary.ca; Tel: 1-403-220-6432)

Abstract

Here we show that pulsed laser-induced dewetting (PLiD) of a thin Au metallic film on a nano-scale ordered dimpled tantalum (DT) surface results in the formation of a high quality Au nanoparticle (NP) array. In contrast to thermal dewetting, PLiD does not result in deformation of the substrate, even when the Au film is heated to above its melting point. PLiD causes local heating of only the metal film and thus thermal oxidation of the Ta substrate can be avoided, also because of the high vacuum (low pO_2) environment employed. Therefore, this technique can potentially be used to fabricate NP arrays composed of high melting point metals, such as Pt, not previously possible using conventional thermal annealing methods. We also show that the Au NPs formed by PLiD are more spherical in shape than those formed by thermal dewetting, likely demonstrating a different dewetting mechanism in the two cases. As the metallic NPs formed on DT templates are electrochemically addressable, a longer-term objective of this work is to determine the effect of NP size and shape (formed by laser vs. thermal annealing) on their electrocatalytic properties.

Keywords: Dimpled Tantalum, Pulsed laser-induced dewetting, Thermal dewetting, Thin gold films, Nanoparticle array

Introduction

The fabrication of metal nanoparticle (NP) arrays has become an active area of research due to their potential applications in patterned magnetic memory arrays[1], catalytic arrays for the growth of semiconductor nanowires and carbon nanotubes[2, 3], and as model electrodes for electrocatalyst evaluation[4, 5]. The construction of metallic NPs of controlled size, spacing, and ordered distribution is essential to the development of these applications. However, it is very challenging to precisely and efficiently arrange individual nanostructures into desired patterns with controlled periodicity, particularly over large areas (i.e., > 1 cm^2)[6].

The fabrication of metal NP arrays can be accomplished by either wet chemical methods involving self-assembly, or lithography-based nanopatterning. Some of the self-assembly processes include dip-coating, spin-coating, and the use of Langmuir-Blodgett methods[7]. In these approaches, the NPs may be deposited on a substrate, but the long-range order within these arrays is limited. On the other hand, lithography techniques, such as electron beam[8], focused ion beam[9], and scanning probe[10] lithographies, allow well-defined and well-positioned NPs to be synthesized.

Metallic NPs can form on solid surfaces by the spontaneous dewetting of thin metastable metal films on various substrates.[11] In this process, an initially smooth film on a solid substrate undergoes morphological changes to reduce the free energy of the ambient film-substrate system, finally breaking up into multiple particles.[7,12-17] However, the dewetting of polycrystalline metallic thin films on flat surfaces usually results in a broad distribution of particle size and spacing.[16] Therefore, significant efforts have been

focused on controlling the dewetting process to fabricate metal NP arrays using nano-templated substrates, normally produced by some form of lithography, e.g., Au[14] or Co[7], on pre-patterned oxidized silicon surfaces. However, these approaches have all required the use of a mask, fabricated using interference lithography.[7, 14]

We have recently reported a simple, versatile, and controlled metallic thin film dewetting protocol in which a highly ordered Au nanoparticle array[12, 13] was deposited over a large area using a highly ordered, self-assembled array of inverted hemispherical caps, or nanodimples,[18-21] as the templating substrate. The dimpled Ta (DT) template, covered with a very thin (3-4 nm) layer of Ta oxide, was formed by the anodization of polycrystalline Ta in a H_2SO_4 + HF solution,[18-20] after which a thin Au film was sputter-coated on the DT surface, followed by thermal dewetting at temperatures around 500 °C to achieve a single Au NP per dimple. We found this temperature to be high enough to cause thermal mobility of the thin film material, resulting in the formation of Au NPs in the dimples. The dewetting of the thin Au film results from the well-known high interfacial tension of metals on oxide surfaces.

Although the experimental protocol is simple, rapid, and robust, and is applicable to the fabrication of other metallic NP arrays, thin film dewetting via thermal annealing depends in a complex manner on the properties of the metal thin film and the substrate material, especially when using high melting point metals. At elevated temperatures, various surface processes, such as metal-substrate chemical interactions and metal diffusion into the substrate, can significantly influence the dewetting process.[15] For instance, the thermal annealing of Pt thin films, deposited on DT, has not yet successfully

produced a Pt NP array due to the high temperatures needed for annealing combined with trace oxygen in our tubular furnaces, thus causing thermal deformation of the DT template as it is oxidized and Pt diffusion into the DT substrate.

In order to avoid these complications of the thermal dewetting process, we report here for the first time pulsed laser-induced dewetting (PLiD) of Au thin films on DT substrates, successfully forming a Au NP array, with the Au NPs sitting neatly in the dimples. The first PLiD experiments were conducted by Bischof *et al* [22] in 1996. This group studied the dewetting of thin Cu, Au, and Ni films on fused silica substrates, observing that, at laser fluences above the melting threshold of the metal, the resulting surface morphology showed characteristic features of spinodal dewetting. Other research groups have observed dewetting of Ag and Co on quartz substrates,[15] while several other studies have proposed that laser dewetting can occur only if the fluence is high enough to cause the metal to be heated to its melting point instantaneously during the short pulse duration.[23] Xia and Chou[24] studied PLiD of Au thin films on both flat and nanoimprint-lithographically patterned silica substrates. They observed a more uniform and smaller particle size distribution on the patterned substrate (65.2 ± 10.4 nm) as compared to what was seen on a flat substrate (106.6 ± 55.8 nm).

Here we show that, when a thin Au film is sputter-coated on a DT template and is then irradiated by laser pulses to above the melting threshold of Au, liquid phase-confined retraction is induced, leading to the formation of a Au NP array on the template, with a close to one NP per dimple configuration. When several laser pulses of 9 ns duration were used, the high processing speed not only significantly reduced the

processing time compared to conventional thermal annealing, but also offers a negligible thermal effect on the substrates in the low oxygen pressure environment in the chamber.

The combination of PLiD of Au thin films with our highly ordered DT templates has resulted in the formation of the smallest nanoparticles formed in an ordered array using thin film dewetting on a patterned substrate.[11, 14, 16] Furthermore, PLiD seems to result in nearly spherical nanoparticles, similar in shape to those used in applications such as electrocatalysis/photo-electrocatalysis. These nearly spherical particles, which are thermodynamically very stable and are not likely to agglomerate on the DT template, can now be used as model electrodes for the determination of NP size effects in electrocatalysis and in the growth of semiconductor nanowires.

Experimental Details

Materials. H_2SO_4 (95−98%), acetone, and isopropanol (all ACS reagent grade) were purchased from EMD Chemicals, while HF (48-51%, ACS reagent grade) and Ta foil (99.95%, 0.127 mm) were obtained from Alfa Aesar. All chemicals were used as received without any further purification and all solutions were made using deionized water (Corning Mega-Pure system). The metal target used for sputtering was high-purity Au (99.99%), obtained from Refining Systems, Inc.

Dimpled Ta template fabrication. Ta specimens (up to 13 mm × 6 mm in size) were cut from as-received Ta foil and were then carefully rinsed, sequentially, with acetone, 2-propanol, and deionized water. Ta anodization was then carried out to form the dimpled

surface, using a Princeton Applied Research 263A potentiostat at a constant voltage of 15 V *vs*. the counter electrode (Pt gauze) for 10 min. A magnetically stirred, room temperature (~23 ^{o}C) solution of concentrated H_2SO_4 (ca. 16 M), containing 3 M HF, was employed for Ta anodization. The Pt counter electrode (CE), placed at a distance of 1 cm from the Ta electrode, was also used as the reference electrode (RE), as conventional REs cannot tolerate the aggressive anodizing solution employed here. Immediately after (within 5 sec) anodization was complete, the samples were rinsed with copious amounts of deionized water and then dried using a stream of N_2 gas (purity 99.998%, PRAXAIR).

Chemical polishing of Ta. Ta specimens (up to 10 mm × 5 mm in size) were cut from as-received Ta foil, rinsed sequentially with acetone, 2-propanol, and deionized water, and were then submerged for 1 - 2 min in a magnetically stirred solution of concentrated HNO_3 (68-70%) + HF (48%) in a volumetric ratio of 1:1. The samples were then rinsed with deionized water and then dried using a stream of N_2 gas.

Metal sputtering. Au thin films (2 - 5 nm thick) were then sputter-deposited onto a dimpled or chemically polished Ta surface using a BAL-TEC SCD 500 sputter-deposition system, with the film thickness established by a BAL-TEC QSG 100 quartz crystal film thickness monitor. The pressure of the high purity Ar gas (99.998%, PRAXAIR) was controlled in the range of 4 - 8 mTorr.

Thermal dewetting (annealing). The Au sputter-coated samples were annealed under N_2 (Purity 99.998 % or 99.7 %, PRAXAIR) in a tube furnace at 500 - 900 °C for 30 min. A

temperature ramp of 60 °C/min was used to reach the annealing temperature, and after annealing was complete, the furnace was allowed to cool down to room temperature in the same gas before removing the sample.

Laser dewetting. Laser radiation with a wavelength of 500 nm and a pulse width of 9 ns from a dye laser (Sirah, CSTR-LG-24), pumped by the third harmonic (355 nm) output of a Q-switched Nd:YAG laser (Spectra-Physics, PRO-250-10) with a repetition rate of 10 Hz, was used to dewet the Au thin films in a vacuum chamber maintained at ~2×10^{-7} Torr by a diffusion pump. The visible beam was directed by a set of prisms through a quartz window into the vacuum chamber. The unfocussed laser, with a spot area of 0.1 cm^2, was directed normal to the Au film on its Ta substrate. Photographic paper was typically used to check the exact position of the laser spot on the Au films.

Surface characterization methods. Field emission scanning electron microscopy (FESEM) was carried out using either a Ziess Sigma VP Field Emission Scanning Electron Microscope (FESEM), or a JOEL JAMP 9500F Field Emission Auger Microprobe, under ultra-high vacuum conditions (< 10^{-10} Torr) and using an electron energy of 20.0 keV. Atomic force microscopy (AFM) analysis was carried out in contact mode (CM-AFM) with a Veeco Nanoscope V, using a phosphorus (n) doped silicon (P:Si) cantilever (RTESPA, Bruker) with a resonance frequency in the range of 345 - 384 kHz and a spring constant of 20 - 80 N/m. The AFM images were evaluated with WSxM5.0 image analysis software[25].

Results and Discussion

(a) Fabrication of dimpled tantalum (DT) templates by electrochemical anodization

Fig. 1 shows a SEM image of a Ta foil surface after 10 minutes of anodization in a HF/H_2SO_4 solution.[18, 19, 21] The surface, which is coated with a very thin (3-4 nm) layer of Ta oxide, is composed of a very uniform, hexagonally arranged, array of dimples, 8 - 10 nm in depth and having an ultrahigh density (~4×10^{10} cm^{-2}), consistent with what has been reported from AFM [18] and cross-sectional transmission electron microscopy (TEM) studies.[26] The dimple diameter and density are both a function of the applied voltage,[13] where the dimple diameter increases and thus the dimple density decreases as the applied voltage increases. While a DT surface is known to be obtainable at anodization voltages between 10 and 20 V, the best monodispersity and long-range order are obtained at an anodization voltage of about 15 V[18], giving a dimple diameter of ~35 nm. The dimpled Ta (DT) surfaces extend over macroscopic distances that are limited only by the substrate size, with the samples used in this study ranging up to 1 cm^2 in area.

(b) Limitations of NP array formation by thermal dewetting on DT templates

We have recently shown that DT surfaces can be used as templates for NP array fabrication,[12] where a Au thin film (3 - 4 nm thick), sputter-coated on a DT surface, was converted into a NP array (Fig. 2) when thermally annealed at 450 – 500 °C in a H_2 or N_2 environment. The dewetting of the thin Au film and subsequent formation of the NPs arises from the well-known high interfacial tension of metals on oxide surfaces. Although

the experimental protocol is simple, rapid, and robust, and is applicable to the fabrication of other metallic NP arrays, thermal dewetting is limited to low melting point (*i.e.,* lower than ~1200 ^{o}C) metal thin films. At elevated annealing temperatures (> 900 ^{o}C), required for the formation of high melting point (> 1200 ^{o}C) metallic NPs, various surface processes, such as metal-substrate chemical interactions and metal diffusion into the substrate, can significantly influence the dewetting process.[15]

Another challenge in forming high melting point NP arrays using DT templates is the thermal oxidation of the substrate that takes place at elevated temperatures and results in substrate volume expansion, ultimately causing surface deformation of the template. Ta is known to thermally oxidize at temperatures ≥ 500 °C when heated in the presence of oxygen or steam,[27] and, the higher the O_2 partial pressure in the annealing environment, the less thermal energy is needed for thermal oxidation and subsequent surface deformation to occur.

We thus investigated the effect of the thermal annealing temperature on the DT morphology (in the absence of a metal coating) in an inert (N_2) environment. Figs. 3a and 3b show FESEM images of DT after annealing for 30 min under low purity N_2 (99.7%) conditions at 500 and 600 °C, respectively. It can be seen that some surface deformation took place even at 500 °C. This surface deformation/oxidation is not seen during the formation of Au NP arrays, as the annealing temperature needed to cause Au dewetting is only around 450 °C.

When a high purity N_2 (99.998%) environment was used for the thermal annealing of a metal-free DT substrate, no sign of surface deformation was observed up to 800 °C (Figs. 3c and 3d). The survival of the DT microstructure under these annealing conditions is likely due to the use of high purity N_2 gas (< 5 ppm O_2 and < 3 ppm H_2O). Even so, DT surface deformation was observed after annealing in N_2 at 900 °C (Fig. 3e), presumably as a result of the increased rate of oxidation of the Ta substrate at this higher temperature.

(c) Au NP array formation via pulsed laser-induced dewetting (PLiD)

In order to make DT-templated NP array fabrication suitable for high melting point metals, we turned to the pulsed laser-induced dewetting (PLiD) technique as a tool for NP formation on DT surfaces. One of the main advantages of this method is that the annealing process takes place under high vacuum, *i.e.,* in the presence of very little oxygen. The pulsed laser also generates only local heating at the substrate surface, *i.e.,* mainly within the coated metal film, in this case. These two advantages should result in annealing without DT substrate deformation by thermal oxidation, thus allowing for the fabrication of DT-supported NP arrays composed of high melting point metals. As a proof of principle, we studied the formation of Au NP arrays on DT substrates using PLiD, with the laser fluence being high enough to produce surface heating above the melting point of Au.

It has been reported that nanosecond pulsed laser irradiation can melt thin metal films, including Au, and convert them into NPs on flat surfaces.[15] For example, a laser

fluence of 194 mJ·cm^{-2} was demonstrated to provide sufficient energy to melt a 10 nm thick Au metal film, even when only a single pulse was used.[24] In this process, the photo-thermal interaction between the laser and the substrate induces distinct local heating of the surface, so that the absorbed laser energy can be considered as being directly transformed into heat.[28]

Here, Au thin films were sputter-coated on DT substrates and then irradiated with laser pulses to reach a temperature above the metal melting threshold, inducing liquid phase confined retraction. With the aid of the templated substrate, a metallic NP array should thus ultimately form. Previous studies[12, 13] showed that the optimum film thickness required for the formation of a Au NP array on a DT surface by thermal annealing is 3 - 4 nm. Therefore, in this work, Au film thicknesses within the range of 2 - 5 nm were used.

Fig. 4a shows a SEM image of a DT surface after sputter-deposition of a ~3 nm Au film using a Au sputter-deposition rate of ~ 11 nm/min and short deposition times (typically 15 - 20 s). It can be seen that, under these conditions, the as-sputtered Au-coated surface has retained the DT topography, indicating that the Au layer was coated smoothly and continuously on both the mesas and dimples prior to annealing. Clearly, the sputtered film shown in Fig. 4a was thick enough to be continuous, and yet sufficiently thin to retain the dimpled contours of the Ta substrate.

When a Au film of ~ 2 nm in thickness was exposed to 10 laser pulses with a fluence of 300 mJ·cm^{-2}, multiple Au NPs (< 10 nm in dia.) were formed per dimple (Fig. 4b). It is thus seen that, if the sputtered Au film is too thin, upon laser exposure,

dewetting occurs at random sites rather than specifically at the dimple edges (mesas), resulting in a lack of order in the NP location and size.

It is important to recall the mechanism of PLiD, in which a substrate surface is irradiated with a laser pulse and the pulsed laser energy is confined within the attenuation length, *i.e.,* near the surface. The conversion of laser energy into heat and the subsequent conduction of the heat into the substrate establishes the temperature distribution in the material. It has been reported that the temperature reached in a Au thin film (10 nm) when irradiated by a single laser pulse of 20 ns at 308 nm was higher than the Au melting point (1064 °C).[24]

Fig. 4c shows that an ordered array of Au NPs (average diameter of 24 nm, as indicated in the histogram in Fig. 4e) was formed upon the exposure of a 3 nm thick Au film, sputter-coated on DT, to 10 laser pulses with a fluence of 300 $mJ \cdot cm^{-2}$. This thin Au film retains the DT morphology, while still allowing the material on the mesa to diffuse to the valley to form the desired highly ordered one particle per dimple configuration. Although there are some defects present in this particular NP array (Fig. 4c), including a few small NPs positioned between dimples, the majority of the NPs in Fig. 4c are of very similar size and are centered in the dimples, as desired. The small Au NPs seen between the dimples may have resulted from non-uniformity of the as-deposited Au film thickness (regions where the film thickness was < 3 nm, e.g. 2.0-2.5 nm, can result in the formation of small NPs, as shown in Fig. 4b).

Due to the fact that these nanoparticles formed after heating the metallic thin film above the melting temperature, although for an extremely short period of time, the

resulting nanoparticles appear to be spherical in shape, which is the lowest energy state. The nanoparticles obtained here are similar in shape to those used in applications such as electrocatalysis/photo-electrocatalysis. Also, another advantage of using dimpled Ta as the substrate is that the overlying metal nanoparticles, formed by dewetting, are electrochemically addressable without any distortion of the electrochemistry by the thin surface oxide of DT, which separates the NPs from the DT substrate.[13] Thus, these arrays can be used, for instance, as model electrodes for the evaluation of nanoparticle size effects on the electrocatalytic activity of relevant electrocatalytic reactions, such as oxygen reduction, hydrogen evolution, and methanol oxidation.

To prove that the DT template causes the thin film laser dewetting process to produce an array of monodisperse NPs, a 2.8 nm thick Au film was deposited on a chemically polished Ta surface (a smooth surface with no dimples). Fig. 4f shows that nanoparticles of a broad size distribution (10 - 60 nm) were formed upon the exposure of the Au film to 10 laser pulses with a fluence of 260 $mJ \cdot cm^{-2}$. The formed NPs are also randomly distributed on the surface, which confirms the importance of using the DT surface to control the size and location of the NPs, as was done for the sample shown in Fig. 4c.

Fig. 4d shows that the laser-induced dewetting of a 4.5 nm thick Au film on a DT surface results in the formation of Au NPs of random size (20 to 80 nm range) and distribution. This indicates that this Au film is too thick to retain the DT morphology[14] and thus, when melted upon exposure to laser irradiation, the films rupture at any defect present in the film surface and not necessarily at the mesas[12] of the DT substrate. In order

to confirm that the DT template morphology has no effect on the dewetting of the Au film when it is ≥ 4.5 nm in thickness, a Au film of similar thickness was sputter-coated on a chemically polished Ta substrate followed by laser irradiation under the same conditions. Fig. 4g shows that Au NPs have formed, with the NPs having the same size distribution as those formed on DT. This indicates that, if the Au film thickness is ≥ 4.5 the film does not interact with the DT template, *i.e.,* the distribution of NPs is not templated by the nanopattern present beneath it during the dewetting process and NP formation.

Interestingly, it was found that the optimal Au film thickness to produce one NP per dimple differed for the two dewetting methods. Specifically, a 2.8 nm Au film dewetted by PLiD will form NPs sitting neatly in the dimples of the DT substrate, whereas the NPs produced by thermal dewetting are much smaller, so that multiple NPs are found within each dimple, as well as between dimples. Conversely, a 4.5 nm Au film will form NPs that are too large to be templated by the dimples when dewetted by PLiD, but forms NPs sitting neatly in the dimples (one NP per dimple) when thermal detwetting is used.

This must relate to differences in the conditions and fundamental steps of the dewetting process using the two approaches, where thermal dewetting at temperatures < 500 ^{o}C causes the slow thermal diffusion of metal atoms on the substrate surface, while PLiD causes cycles of full melting and re-solidification. Additionally, the shape of the NPs formed by the two different dewetting methods was noted to be quite different. NPs formed by thermal dewetting (Fig. 2) appear to be flatter than those formed by PLiD,

after which the NPs appear nearly spherical in shape in the SEM images (Figs. 4 c, d, f and g).

In order to confirm these shape differences, atomic force microscopy (AFM) analysis was carried out on two different samples, annealed using the two different methods. Au film thicknesses found to lead to templating of the resulting Au NPs in a one NP per dimple configuration were used (2.8 nm Au thin film for laser annealing (Fig. 4c) and 4.5 nm for thermal annealing (Fig. 5b (inset)). If the two annealing methods result in NPs of similar shape, the thicker thermally annealed Au film should produce NPs with a larger height than seen for the thinner laser annealed Au film.

Fig. 5a shows an AFM image of the Au NPs produced via PLiD, where the distance between neighboring particles is ~ 50 nm. This confirms that these NPs are located in the dimples as the center-to-center distance of dimples is also ~ 50 nm. The average height of the NPs is 9.5 nm (4.5 nm from the mesa to particle top, plus 5 nm from dimple valley to mesa[18]), as indicated by the line profile (Fig. 5c), and the average particle diameter, determined from the SEM images, is 21.4 ± 4.4 nm, *i.e.*, an aspect ratio (height/width in a top down view) of ~ 0.44. The average height of the NPs formed by PLiD may in fact be slightly more than 9.5 nm, as the AFM tip will not reach the surface of the mesas between NPs (with the possible exception of the feature at 190 nm in Fig. 5c), thus making it possible to deduce only that the NPs are at least 4.5 nm above the dimple mesas.

In contrast, the AFM analysis of the thermally annealed sample revealed that Au NPs have lower aspect ratios than described above for the PLiD formed NPs, although

the annealed film is thicker in this case. The average height of the NPs is about 6.5 nm (1.5 nm from mesa surface to top of the Au NP plus 5 nm distance from valley to mesa), as indicated by the line profile (Fig. 5d) and shown on the corresponding AFM image (Fig. 5b). Figs. 5b and 5d show both the NPs and dimple mesas, as indicated by the ~30 nm spacing between the high points in the AFM line profile. The average particle diameter measured from the corresponding SEM image is 31.0 ± 2.1 nm (inset of Fig 5b), thus yielding an aspect ratio of ~ 0.21, which is significantly lower than that of the NPs produced via PLiD. This confirms that the PLiD method results in NPs that are more spherical in shape than those obtained via thermal annealing under the conditions used in this study.

Finally, as the local temperature of the Au film as a result of laser irradiation is higher than the melting point of Au, this work clearly demonstrates that the pulsed laser dewetting technique can be safely used with DT templates in order to fabricate NP arrays composed of metals with high melting points. In a parallel work on pulsed laser dewetting of Pt thin films on DT, Pt NP arrays were also successfully achieved[29]. In contrast to the more conventional thermal annealing technique,[13] this can be achieved using the PLiD method without inducing surface deformation during annealing as a result of the thermal oxidation of the substrate, such as the Ta metal used in the present work.

Conclusions

This work illustrates the feasibility of the controlled fabrication of monodisperse metallic (Au) nanoparticles (NPs) on pre-patterned surfaces by using pulsed laser-

induced dewetting (PLiD). This method relies on the formation of Au NPs via confined thin Au film dewetting on a highly ordered dimpled tantalum (DT) surface fabricated by a simple electrochemical method. In contrast to the conventional thermal dewetting approach, which results in the formation of flattened NPs (height/width aspect ratio is 0.21), PLiD produces NPs that are significantly more spherical in shape (aspect ratio 0.44). This can be attributed to the differences in the mechanism of the dewetting process using the two approaches. In thermal dewetting, temperatures of < 500 ^{o}C cause slow thermal diffusion of metal atoms on the substrate surface, which, combined with the interfacial tension between the metal and the oxide layer coating the DT substrate, results in the formation of nanoparticles. In contrast, PLiD causes cycles of full melting and re-solidification of the sputter coated metal.

Additionally, PLiD takes place under a high vacuum, providing a very low pO_2 environment, and generates local heating only near the substrate surface, *i.e.,* primarily within the thin metal film. This results in thin Au film dewetting and the formation of a Au NP array without the deformation of the Ta substrate due to its oxidation. In our earlier studies, we observed significant substrate deformation associated with thin film dewetting via thermal annealing when the annealing temperature is higher than 600 ^{o}C.

The protocol developed here is highly versatile, as it is expected that any metal, deposited as a thin film (~3 nm) on the DT substrate, will form NPs, with one particle per dimple, by pulsed laser-induced dewetting. This is the result of the well-known high interfacial tension of metals on Ta oxide. Fortunately, Ta is also a very high melting point

metal (> 3000°C), and thus a wide range of metals and alloys can be dewetted on the DT substrate without disturbing the DT morphology. This further increases the applicability of our NP array fabrication approach. These arrays have many applications, including in magnetics, plasmonics, surface enhanced Raman spectroscopy and other photonic devices, as well as for many electrochemical purposes.

Acknowledgements

The authors gratefully acknowledge the Natural Sciences and Engineering Research Council of Canada for financial support of this work and Alberta Innovates - Technology Futures for scholarship support of CAH. Thanks are also extended to Drs. Dimitre Karpuzov and Shihong Xu at the Alberta Centre for Surface Engineering and Science (ACSES, University of Alberta) for their assistance with the FESEM and other surface analysis methods.

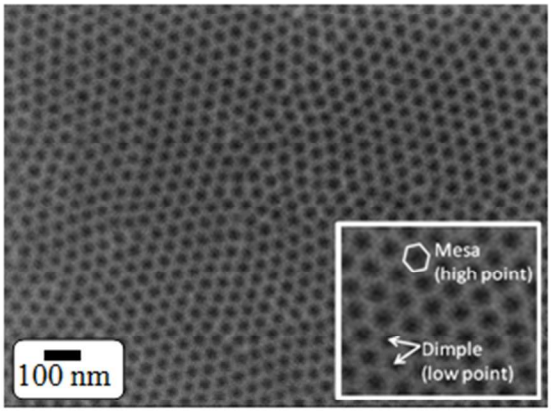

Fig. 1: Plane view FESEM images of DT fabricated by 10 min of Ta anodization in a 16 M H_2SO_4 + 3 M HF solution at 15 V *vs.* a Pt counter electrode.

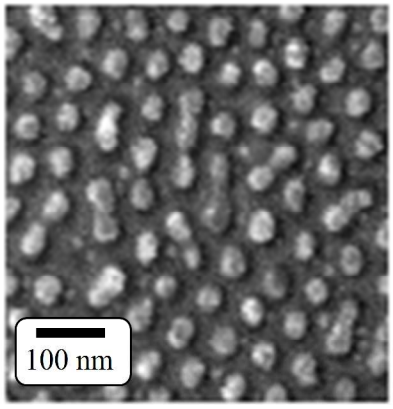

Fig. 2: Plane view FESEM image of Au nanoparticle array formed on a dimpled Ta surface by thermal dewetting.

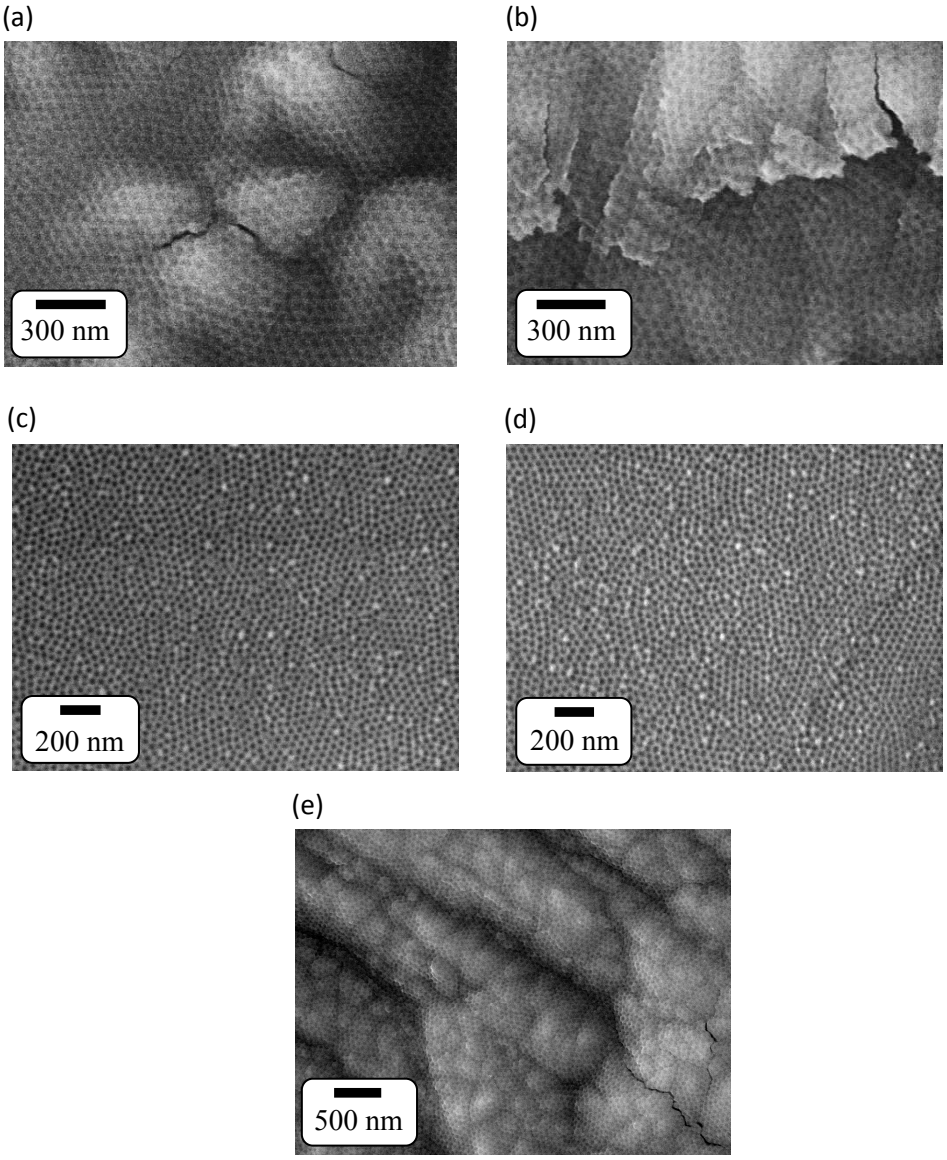

Fig. 3: Plane view FESEM images of DT, thermally annealed for 30 min under 99.7 % purity N_2, at (a) 500 °C and (b) 600 °C, and under 99.998 % purity N_2 at (c) 700 °C, (d) 800 °C, and (e) 900 °C.

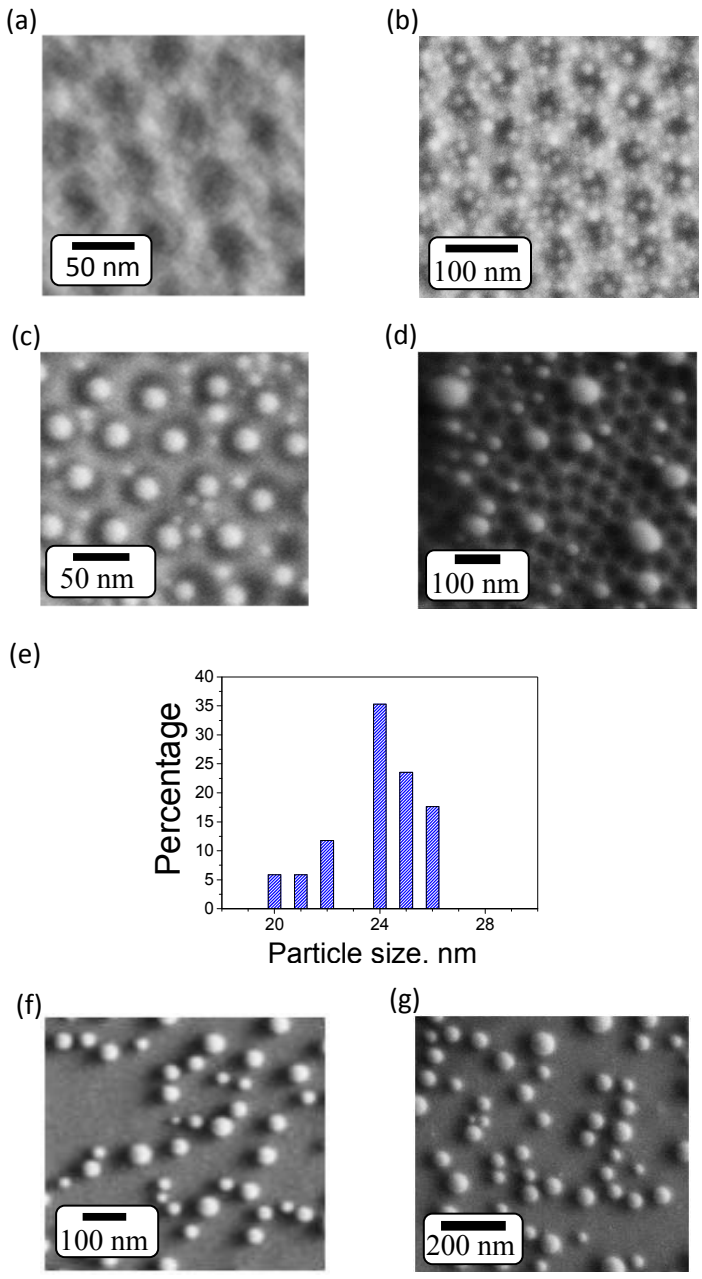

Fig. 4: Plane-view FESEM images of Au thin films of a variety of thicknesses, sputter-deposited on dimpled Ta (DT) before (a) and after laser-dewetting (b, c, and d). The thickness of the sputtered films is (a, c) 2.8 nm, (b) 1.9 nm, and (d) 4.5 nm, while (e) shows a histogram of the particle size distribution resulting from the dewetting of a 2.8 nm (c) thick Au film on the DT surface. The images in (f) and (g) are for 2.8 and 4.5 nm, respectively, Au films after laser-dewetting from a chemically polished Ta substrate. The Au film thickness clearly has a dramatic effect on the morphology of the nanostructures formed upon annealing.

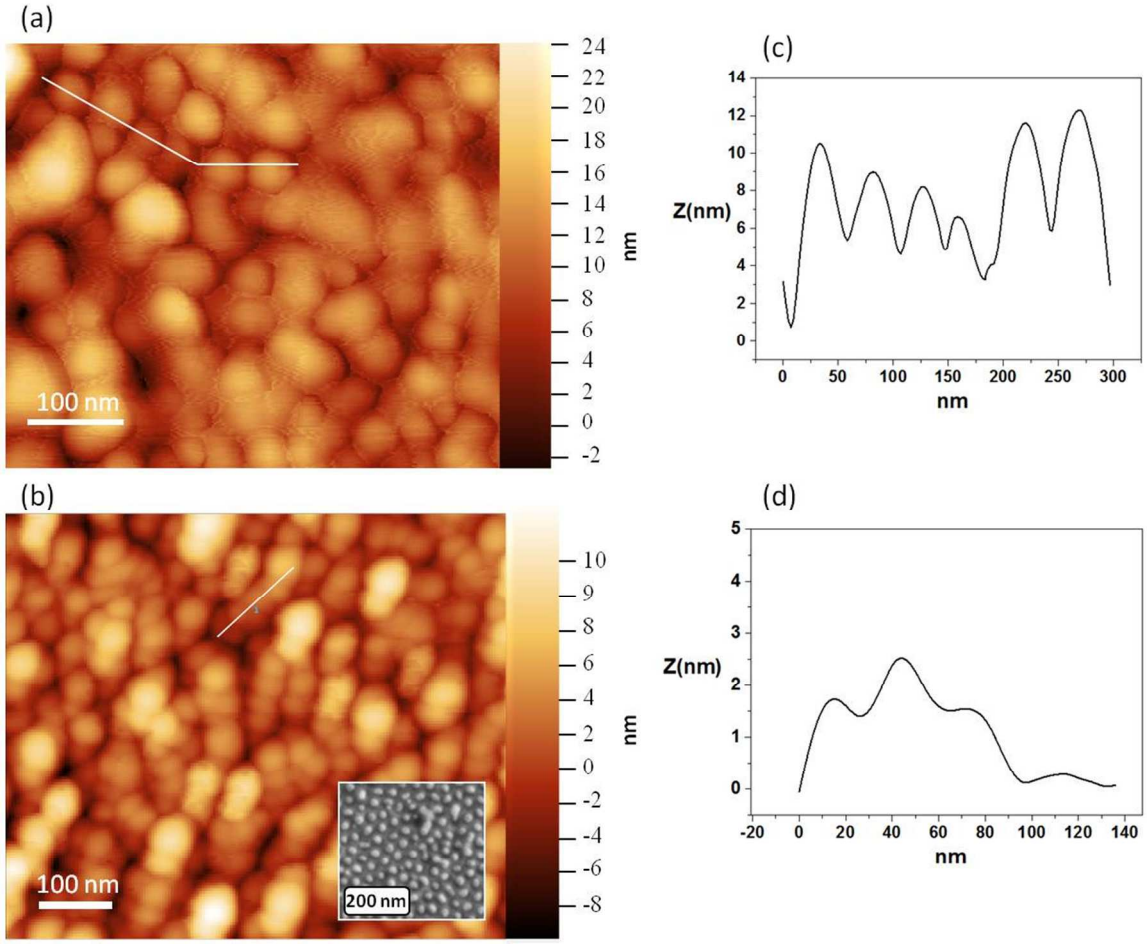

Fig. 5: AFM images of (a) 2.8 nm Au thin film on DT substrate after laser-induced dewetting and (c) the corresponding line profile, and (b) 4.5 nm Au thin film on DT after thermal annealing and (d) the corresponding line profiles.

References

1. W. Lee, H. Han, A. Lotnyk, M. A. Schubert, S. Senz, M. Alexe, D. Hesse, S. Baik and U. Gosele, *Nat Nanotechnol*, 2008, 3, 402-407.
2. M. C. Plante and R. R. LaPierre, *J Cryst Growth*, 2008, 310, 356-363.
3. A. A. Puretzky, D. B. Geohegan, S. Jesse, I. N. Ivanov and G. Eres, *Appl Phys A-Mater*, 2005, 81, 223-240.
4. Y. L. Gu, J. St-Pierre and H. J. Ploehn, *Langmuir*, 2008, 24, 12680-12689.
5. M. Gustavsson, H. Fredriksson, B. Kasemo, Z. Jusys, J. Kaiser, C. Jun and R. J. Behm, *J Electroanal Chem*, 2004, 568, 371-377.
6. J. Li, K. Kamata and T. Iyoda, *Thin Solid Films*, 2008, 516, 2577-2581.
7. Y. J. Oh, C. A. Ross, Y. S. Jung, Y. Wang and C. V. Thompson, *Small*, 2009, 5, 860-865.
8. C. R. K. Marrian and D. M. Tennant, *J Vac Sci Technol A*, 2003, 21, S207-S215.
9. T. Nagata, P. Ahmet, Y. Sakuma, T. Sekiguchi and T. Chikyow, *Appl Phys Lett*, 2005, 87, 013103.
10. D. S. Ginger, H. Zhang and C. A. Mirkin, *Angew Chem Int Edit* 2004, 43, 30-45.
11. Y. Kojima and T. Kato, *Nanotechnology*, 2008, 19, 255605.
12. H. A. El-Sayed and V. I. Birss, *J Mater Chem*, 2011, 21, 18431-18438.
13. H. A. El-Sayed, H. M. Molero and V. I. Birss, *Nanotechnology*, 2012, 23, 435602.
14. A. L. Giermann and C. V. Thompson, *Appl Phys Lett*, 2005, 86, 121903.
15. H. Krishna, N. Shirato, C. Favazza and R. Kalyanaraman, *J. Mater. Res.*, 2011, 26, 154-169.
16. D. Wang, R. Ji and P. Schaaf, *Beilstein J. Nanotechnol.*, 2011, 2, 318-326.
17. K. Zhao, R. S. Averback and D. G. Cahill, *Applied Physics Letters*, 2006, 89, 3.
18. H. El-Sayed, S. Singh, M. T. Greiner and P. Kruse, *Nano Lett*, 2006, 6, 2995-2999.
19. H. El-Sayed, S. Singh and P. Kruse, *J Electrochem Soc*, 2007, 154, C728-C732.
20. H. A. El-Sayed and V. I. Birss, *Nano Lett*, 2009, 9, 1350-1355.
21. H. A. El-Sayed and V. I. Birss, *Nanoscale*, 2010, 2, 793-798.
22. J. Bischof, D. Scherer, S. Herminghaus and P. Leiderer, *Physical Review Letters*, 1996, 77, 1536-1539.
23. J. Trice, D. Thomas, C. Favazza, R. Sureshkumar and R. Kalyanaraman, *Physical Review B*, 2007, 75, 235439.
24. Q. Xia and S. Y. Chou, *Nanotechnology*, 2009, 20, 285310.
25. I. Horcas, R. Fernández, J. M. Gómez-Rodríguez, J. Colchero, J. Gómez-Herrero and A. M. Baro, *Review of Scientific Instruments*, 2007, 78, 013705.
26. S. Singh, W. R. T. Barden and P. Kruse, *ACS Nano*, 2008, 2, 2453-2464.
27. K. C. Saraswat, R. S. Nowicki and J. F. Moulder, *Appl Phys Lett*, 1982, 41, 1127-1129.
28. M. S. Brown and C. B. Arnold, in *Fundamentals of Laser-Material Interaction and Application to Multiscale Surface Modification*, Springer, 2010, vol. 135, pp. 91-120.
29. E. Owusu-Ansah, C. A. Horwood, H. A. El-Sayed, V. I. Birss and Y. J. Shi, *submitted*, 2015.